

Numerical Analysis of S175 Container Ship Motion under Irregular Wave by HOS-CFD Method

Jian Guan, Yuan Zhuang, Jianhua Wang*, Decheng Wan

Computational Marine Hydrodynamics Lab (CMHL), School of Naval Architecture, Ocean and Civil Engineering,
Shanghai Jiao Tong University, Shanghai, China

*Corresponding author

ABSTRACT

In this paper, the research of S175 ship sailing under long-crested irregular waves is conducted with the application of coupling CFD solver naoe-FOAM-SJTU-os and HOS method. The encountering of the bow with largest wave trough, largest wave crest and largest wave height is considered. The verification of the present method is carried out through the ship motion under regular wave, compared with available experimental results. Then, the motion and slamming load results of the CFD simulation is analyzed. For the ship motion, the encounter of S175 ship and extreme wave moments enlarges heave and pitch motion, the latter shows better stability and larger amplitude after the encounter. For the slamming load, two slamming peaks are captured in the whole slamming process and the two peaks show distinguished differences in both spatial dimension and time dimension. Moreover, green water phenomenon is observed which is most severe under the encounter of the largest wave crest and the S175 ship. The conclusion is drawn that the encounter of the largest wave crest and bow should be paid great attention to when ship sails in long-crested irregular wave.

KEY WORDS: Irregular wave; HOS-CFD method; slamming load; ship motion.

INTRODUCTION

The globalization advances the global sailing industry that the design of voyage and load ability of container ships continuously increases to satisfy the demand of global trade. The safety of large ships is of great concern since the scale of ships themselves affect their seakeeping and the complex sea conditions poses threats to the sail safety as well. For example, the long-crested waves are risky for large container ships since the wave length is on the same scale as the ship length, and the slamming loads demonstrate strong nonlinearity. Official standards, model experiments and numerical simulations are comprehensively applied in the evaluation of the sailing safety. To name just a few, ABS (American Bureau of Shipping) published standard for slamming loads and strength assessment for vessels. Kim et al. (2019) conducted experiments of a

10,000 TEU under comprehensive wave conditions. Wang et al. (2023) simulated motions and slamming loads under oblique regular waves using solver naoe-FOAM-SJTU. To be mentioned, the numerical simulation is undergoing rapid development due to the progress of calculation hardware and the flexibility and advantages in time and fund cost itself.

For ship motion simulation in complicated sea conditions, three main technique routes are popular in naval CFD industry: potential method (Shi et al., 2024), viscous method (Tezdogan et al., 2016) and potential-viscous-coupled method (Yu et al., 2023). The coupling of potential and viscous method combines the rapid of complicated wave generation of potential method and the accuracy of viscous method in fluid field simulation.

For wave generation, besides the original wave generation module of OpenFOAM, waves2Foam (Jacobsen et al., 2012) is applied in numerous researches. The wave generation and absorption are realized with either relaxation zone (Karola et al., 2024) or generating-absorbing boundary condition (GABC) (Zhao et al., 2024).

For irregular wave conditions, the HOS method which is utilized in this research is more frequently applied. HOS method is based on the potential theory of wave, which can simulate the waves accurately and fast since the potential theory calculation of waves is much more rapid than the viscous calculation of waves, which saves considerable time in simulation. Xiao et al. (2019) analyzed the nonlinearities of focused waves, irregular waves and the subsequent nonlinear effects to ship motions with the utilization of HOS. Zhuang et al. (2023a; 2023b) coupled HOS method with naoe-FOAM-SJTU and verified the method with the interaction of focused wave and a moving cylinder and FPSO in model scale and full scale. Xie et al. (2023) combined HOS method with Smoothed Particle Hydrodynamics (SPH) method, realizing the improvement of computational efficiency and extensive reduction of the numerical dissipation.

In this research, the S175 container ship is chosen as the research target and the ship motion and slamming characteristics under long-crested irregular waves are analyzed. The wave generation is firstly realized through the HOS software HOS-NWT. Then, the wave generation through the coupling of HOS method and naoe-FOAM-SJTU shows good agreement and the results of motion and slamming load

demonstrates distinct features under three wave incident moment: the bow encounters the largest trough, crest and wave height.

NUMERICAL METHOD

naoe-FOAM-SJTU Solver

In this research, the viscous fluid field is simulated by self-developed CFD solver naoe-FOAM-SJTU, which contains modules of 6-DOF motion, wave generation and absorption, and overset method. It is worth noting that the overset module applied in this research utilizes SUGGAR++(Noack, 2005), to create the overset composite grid and realize the interpolation among separate sections of grids with Domain Connectivity Information (DCI).

Governing Equations

The governing equations in this research unsteady incompressible two-phase fluid, the continuity and momentum equations can be written as follows:

$$\nabla \cdot \mathbf{U} = 0 \quad (1)$$

$$\frac{\partial \rho \mathbf{U}}{\partial t} + \nabla \cdot (\rho \mathbf{U} \mathbf{U}) = -\nabla p + \rho \mathbf{g} + \nabla \cdot (\mu \nabla \mathbf{U}) \quad (2)$$

where \mathbf{U} is the velocity field, ρ is the density of the liquid, \mathbf{g} is the gravitational acceleration and μ is the viscosity coefficient. For the turbulence model, $k-\omega$ SST, introduced by Mentor(1994), is chosen for the calculation.

HOS-CFD Method

In this research, the HOS software HOS-NWT, developed by Ducroz et al. (2012), is applied, which can simulate the waves conditions in physical wave tank. The potential method HOS solves potential only around free surface by Laplace equation and represents the nonlinearity by Taylor expansion and the perturbation method. The coupling of HOS and naoe-FOAM-SJTU is realized by Grid2Grid (Choi et al., 2017), an open source package software for HOS which transfer the spectrum result of HOS to time domain result for CFD simulation. Zhuang et al. (2023a) compared the efficiency of the HOS-CFD method with the CFD method in the research of interaction between FPSO and focused wave, indicating that HOS-CFD method can reduce the CPU time to almost ten times less than CFD method.

Fig. 1 is the diagram of the calculation field of HOS and CFD method. The wave information is transformed trough relaxation zone. In terms of overset method, the CFD field can be comprehended that the CFD field moves with the object (S175 ship in this research) while the CFD field moves inside the HOS field which is static.

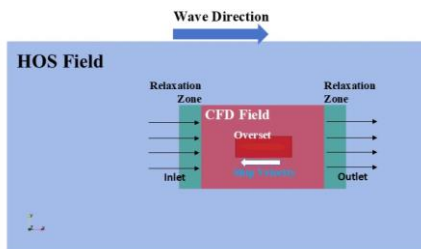


Fig. 1 Diagram of the calculation field of coupling HOS and CFD method

SIMULATION MODEL AND CASES

Geometry

The S175 container ship is chosen as the research object, whose dimension is listed in the following table. In the present research, the scale of the S175 ship model is 1:40.

Table 1 Dimension of S175 container ship

Main dimension	Full Scale	Model
Length L_{pp} (m)	175	4.375
Beam B (m)	25.4	0.635
Depth D (m)	19.5	0.488
Draft T (m)	9.5	0.238
Displacement Δ (t)	23711	0.370
Wetted area S_w (m ²)	5496	3.435
LCG (m)	90.11	2.25
KG (m)	8.5	0.213
$K_{xx}/B, K_{yy}/L_{pp}, K_{zz}/L_{pp}$	(0.380,0.240,0.240)	(0.380,0.240,0.240)
Moment of inertia (kg·m ²)	(0.217,4.417,4.417)e10	(21.158,431.344,31.34)

Numerical Setup and Cases

The simulation domain setup is a composition of HOS field and CFD field, as mentioned in HOS-CFD Method section. The HOS and CFD layout are shown in Table 2 and Fig. 2. To satisfy the requirement of both sufficient propagation of wave and adequate distance for the sail of S175 ship model, the distance of HOS field in x direction is extended to 100m.

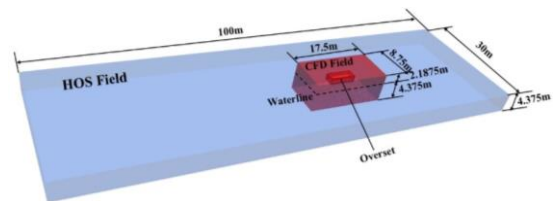


Fig. 2 Simulation domain setup

Table 2 Specific parameters of simulation domain

Section	Parameters (x*y*z) (m)
HOS Field	100*30*4.375
CFD Field (background mesh)	17.5*8.75*6.563
Relaxation Zone (beginning and end of CFD Field in x axis)	4.375*8.75(at z=0m)
Overset	5.906*2.188*1.313

The wave generated by HOS is an irregular wave on the basis of JONSWAP spectrum with the duration of 1500 seconds. The time step of the HOS simulation is 0.01s. The result data of the HOS simulation is about 5.5GB. The peak period T_p is 1.673s and the significant wave height H_s is 0.175m (7 meters in full scale). In this research, it is supposed that the S175 ship arrives at the position of 55 meters in x-direction of the HOS field at the CFD calculation time of 10 seconds and

at the speed of 0.813m/s (10 knots in full scale). The wave elevation history of position (55,0) with long-crest properties are selected for the present research. From them, fragments with the largest wave trough, crest and wave height (the difference of neighboring wave trough and crest) are the target wave fragments, originating three simulation cases. The trough and crest occur at the moment when the S175 ship reaches (55,0) while in terms of the largest wave height, the ship arrives at (55,0) when the wave elevation is zero, which is between the trough before and the following crest. The duration of each desired wave fragment is 15 seconds in order to guarantee the fluid field is fully developed before the encountering moment. The wave cases are listed in Table 3.

Table 3 Cases of present research

Case	Target HOS Time(s)	Wave Feature
1	896.07s	Trough
2	163.87	Crest
3	402.30	Wave Height

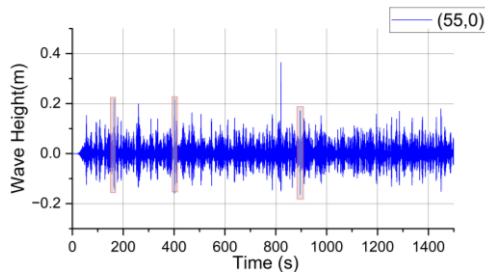


Fig. 3 HOS wave time history of position (55,0) in HOS field and the desired wave fragments

Grid Distribution

In terms of grids, the generation is based on the requirement of accurate capture of free surface. For the irregular wave in this research, 20 grids are arranged in vertical direction along the significant wave height while the vertical interval of fined free surface grids is arranged to cover the largest wave amplitude. The grids along x and y directions are arranged accordingly.

Fig. 4 shows the grids near free surface of background mesh. After determining the background mesh, the arrangement of overset mesh is on the two basics: first, the grids around the hull patch are refined and layers are placed at the surface of the hull for better simulation of turbulence. Second, the grids on the boundary of overset mesh should match these of the background mesh in lengths, with the length ratio less than 1:2 according to the interpolation axis. Take x-y plane as example, the relationship between background mesh and overset mesh is shown in detail in Fig. 5. The grid distribution of the present research is shown in Fig. 6, in which black mesh stands for background mesh and red mesh stands for overset mesh. The final grid setup according to the wave cases in this research is listed in Table 4. The storage of the CFD results in a single time step (0.001s) is about 2.0GB.

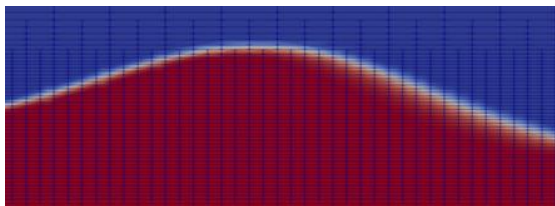


Fig. 4 Grids near free surface

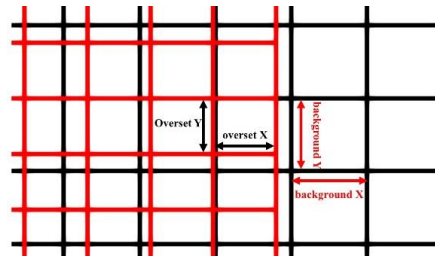


Fig. 5 The length relationship between background and overset mesh



Fig. 6 Grid distribution

Table 4 Grid setup under different wave cases

Case	Background Grid	Overset Grid
1	6.15 million	2.82 million
2	6.60 million	2.88 million
3	6.60 million	2.88 million

Slamming Load Probes

Several slamming load probes are set at bow, with the distribution from bow flare to the bottom of the bow. The position of slamming load probes is listed in Table 5 and shown in Fig. 7.

Table 5 Slamming load probes setup

Position	Probe num.	Coordinate
Bow flare	P1	(0.109,-0.062,0.1)
	P2	(0.219,-0.085,0.1)
Waterline	P3	(0.109,-0.022,0)
	P4	(0.219,-0.036,0)
Beneath waterline	P5	(0.109,-0.027,-0.1)
	P6	(0.219,-0.035,-0.1)
Bottom	P7	(0.109,0,-0.238)
	P8	(0.219,0,-0.238)

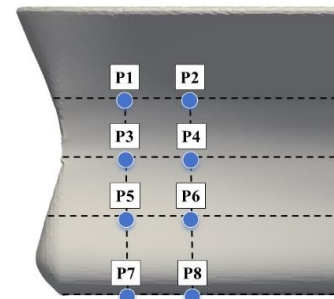


Fig. 7 Slamming load probes setup

REGULAR WAVE VERIFICATION

Before the simulation under irregular wave, the verification of the HOS method in this research is carried out. The simulation case refers to the experiment done by Fonseca & Soares (2004) which measured the motion of S175 ship model which is identical to the one in present research under regular waves. The verification is conducted under the regular wave with the wave length of $1.2 L_{pp}$ and the wave steepness of $1/120$. The Fn of the S175 container ship is 0.25. The grid of verification is under the standard that the grids of free surface should be no less than 12 in vertical direction in order to accurately capture the free surface. The generation of grids of the hull is done accordingly, whose process refers the procedure in the SIMULATION AND CASES section of this paper. The verification of heave and pitch motion in full scale is shown in Fig. 8. The verification results in Fig. 8 agree well with the experimental results, thus the HOS-CFD method in the present research is verified.

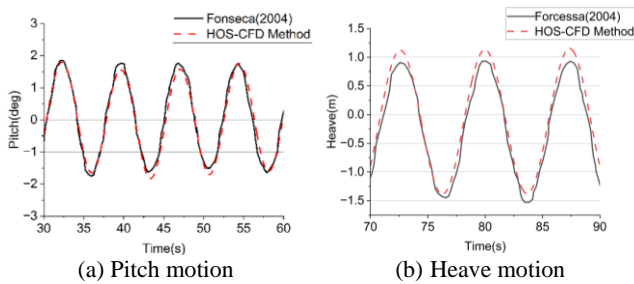


Fig. 8 Verification of ship motion

RESULTS AND ANALYSIS

Motion Responses

The motion responses under three wave conditions are demonstrated in Fig. 9. It should be mentioned that the large motion amplitude at the beginning of Case 3 is due to the initial wave the S175 ship encounters whose wave height is about half of the significant wave height. The motion of S175 ship requires about 2 second to develop to its stable condition, so that the large motion at the beginning of Case 3 is not analyzed. From

Fig. 9, rises of the amplitude of heave and pitch motion can be found after $T=10s$, which indicates that the largest wave trough, crest and amplitude strengthen the motion of ship. Moreover, the large amplitude of heave motion attenuates more rapid than pitch motion. The large amplitude duration of heave motion is less than that of pitch motion by a motion period. Also, the large motion amplitude stability of pitch motion is better. From $T=10s$ to $T=13s$, in Case 1, the amplitude of pitch motion maintains at about 3 degrees while the amplitude of heave motion is changeable, similar phenomenon can be observed in Case 3. In Case 2, despite the relatively stable amplitude of heave motion, it attenuates faster than pitch motion, especially the crest of time history. Briefly, under extreme wave conditions of irregular waves: the largest wave trough, crest and wave height, the ship motion enlarges and maintain for several period, meanwhile the influence to pitch motion lasts longer than heave motion.

Slamming Loads

Fig. 10 and Fig. 11 demonstrates the slamming load time history of 4

positions of the bow in Case1 and Case3. In Case1, the slamming load rises to the largest after $Time=10.5s$ while in Case3, the peak occurs at $Time=10.15s$, about 0.4s after the largest trough of wave, which indicates that slamming reaches the peak 0.5s after the largest trough of wave. However, the development of the slamming load is distinct, depending on not only position of the probes, but also the case. The statistics of slamming load peak are shown in Fig. 12. The distinguishments of the two slamming peaks after the S175 ship encountering the largest wave trough and wave height are summarized in Fig. 13. The peak pressure rises with the decrease of vertical position of probes in both cases. However, the peak pressure increases in Case1 while decreases in Case3. The distinguishment of slamming peak decreases when the slamming probe becomes lower in Case 1, from $-404.7Pa$ in P1 to $-36.5Pa$ in P7, the ratio is approximately 11 times. While in Case3, the distinguishment remains at about 155Pa.

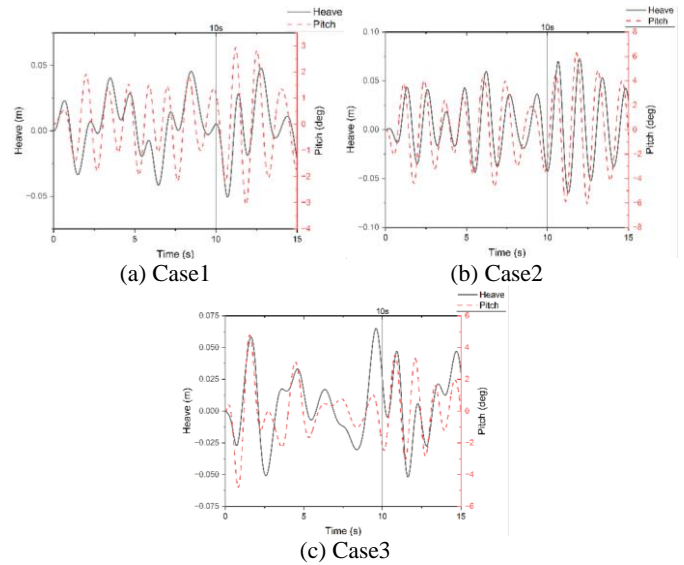


Fig. 9 Ship motion time history

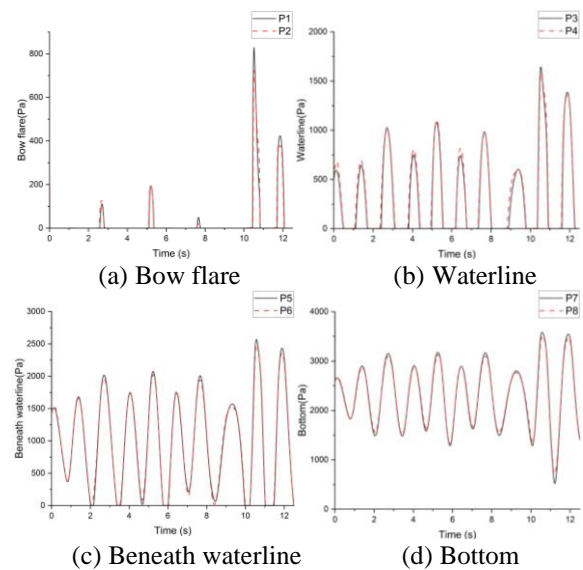


Fig. 10 Slamming load time history of Case1

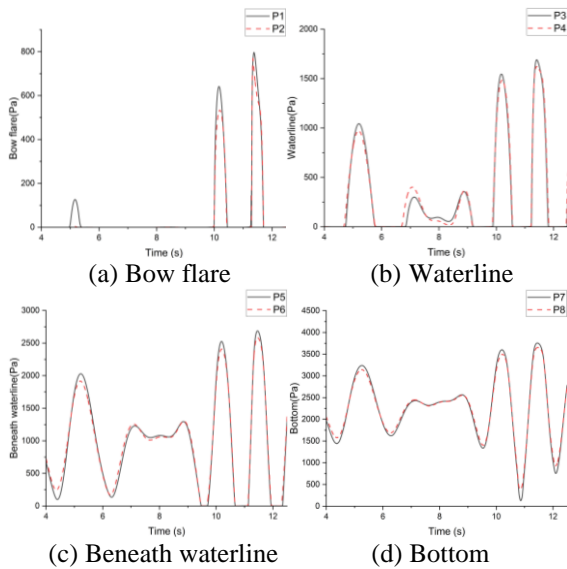


Fig. 11 Slamming load time history of Case3

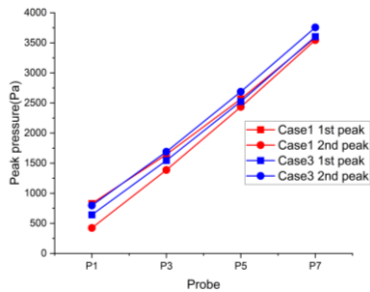


Fig. 12 The statistics of slamming peak

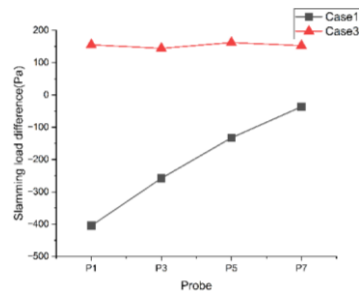


Fig. 13 The difference of slamming peak

Flow Field Analysis

Fig. 13 can be explained by Fig. 14 and Fig. 15, which compare the wave elevation and pressure distribution under two slamming peak moment. For Case 1, the wave elevation at the front of S175 ship is higher under 1st slamming peak moment, which explains the decrease of slamming load at 2nd slamming peak moment. The pitch motions at two peak moments are close, while at 1st peak moment, the S175 ship is near the trough and the free surface near the hull at 2nd peak moment is flat, which results in the inconsistent pressure gradient in the vertical direction of the ship. That phenomenon is the consequence of different encounter case of the ship, which causes the variation of slamming load difference of two peaks in Case1.

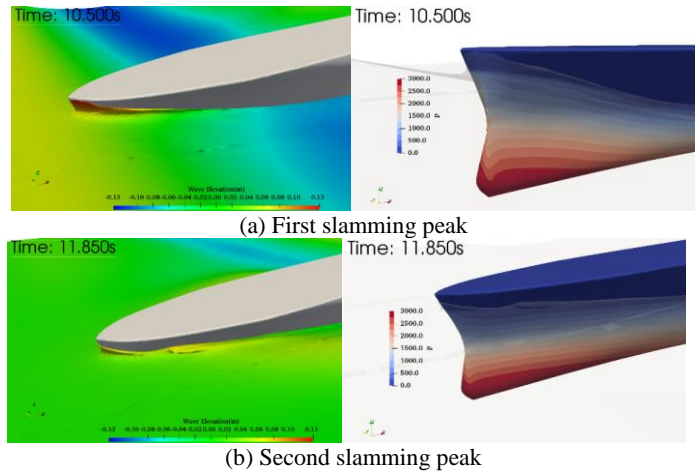


Fig. 14 The wave elevation and pressure distribution in Case 1 at the peak moment of slamming

For Case 3, the S175 ship encounters the large wave crest at the first peak moment while its surrounding free surface is flat at the second peak moment. However, the water elevation is more severe at the second one, which compensates the difference of waterline shape around the bow, resulting in the constant increase of slamming pressure of the 4 probes. The increase in slamming load peak can be explained by the larger wave elevation around the hull.

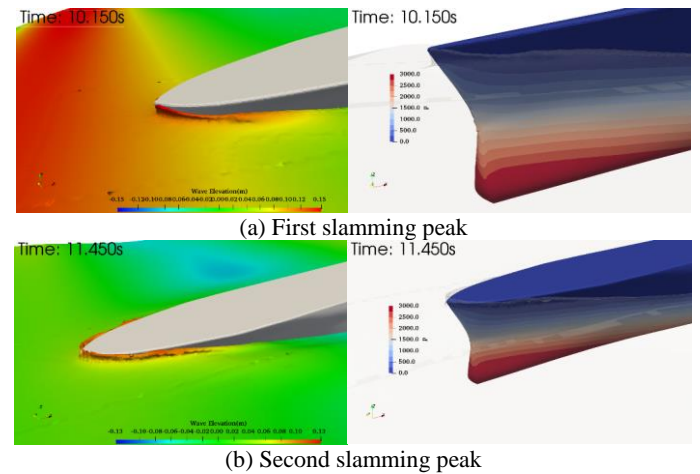


Fig. 15 The wave elevation and pressure distribution in Case 3 at the peak moment of slamming

For Case 2, the results are quite distinct from the 2 cases analyzed above, since the most severe green water phenomenon is observed when the S175 ship encounters the largest crest. The whole ship bottom is above the free surface when the trough comes. However, the pressure distribution around the hull is similar to that in Case 3.

Comparing the wave elevation and the pressure distribution above, three cases demonstrate different properties: (1) Case 1 demonstrates the most oblique gradient of pressure trough vertical direction of the ship at the first slamming peak moment. (2) Case 2 demonstrates the most severe green water phenomenon; thus, this case is the riskiest case when the ship sails in long-crested irregular wave.

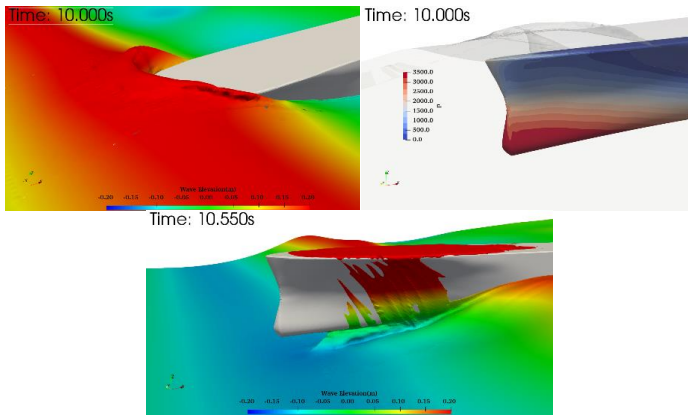


Fig. 16 Severe wave-ship interaction in Case2

CONCLUSION

In this research, the motion and slamming load properties of S175 ship sailing in long-crested irregular wave are simulated and analyzed by the combination of naoe-FOAM-SJTU-os and HOS method. Three different wave conditions during irregular wave evolution are selected as simulation cases. The bow encounters the largest wave trough, wave crest and largest wave height in three cases, named as Case 1, 2, 3 respectively. Wave generation verification of the HOS method is carried out before simulation and the accuracy of the coupling HOS and CFD method is certificated.

The motion of S175 ship is firstly analyzed. The long-crest period of encountering wave strengthens the heave and pitch motions. The pitch motion demonstrates stability and large amplitude longer than the heave motion.

Moreover, in terms of the slamming load, the long-crested waves result in rise of the pressure of the bow. The difference of the first peak and second peak is observed and analyzed. When the S175 ship interacts with the large wave trough, the second peak of slamming shows decrease to the first one, with distinguished difference of slamming load in the vertical direction of the hull. While in the case of encountering large wave height, the second slamming peak shows increase which is mostly consistent in the probes set along the vertical direction of the bow. The encounter of the large wave crest and the S175 ship is the most massive, with the most severe green water phenomenon than the other two wave cases. Thus, it can be concluded that when a ship sails under long-crested irregular waves, the encounter of bow and large wave crest should be most considered and paid attention to.

ACKNOWLEDGEMENT

This work was supported by the National Natural Science Foundation of China (52201372), to which the authors are most grateful.

REFERENCES

- Choi, YM, Gouin, M, Ducrozet, G, and Bouscasse, B (2023). "Grid2Grid: HOS Wrapper Program for CFD solvers," *ArXiv [Preprint]*, 1801.00026.
- Ducrozet, G, Bonnefoy, F, Le Touzé, D, and Ferrant, P (2012). "A modified high-order spectral method for wavemaker modeling in a numerical wave tank," *Eur J Mech B Fluids*, 2012, 34: 19-34.
- Fonseca, N, and Soares, CG (2004). "Experimental Investigation of the Nonlinear Effects on the Vertical Motions and Loads of a Containership in Regular Waves," *J Ship Res*, 48(02): 118-147.
- Jacobsen, NG, Fuhrman, DR, and Fredsoe, J (2012). "A wave generation toolbox for the open-source CFD library: OpenFoam (R)," *Int J Numer Methods Fluids*, 70.
- Karola, A, Tavakoli, S, Mikkola, T, Matusiak, J, and Hirdaris, S (2024). "The influence of wave modelling on the motions of floating bodies," *Ocean Eng*, 306, 118067.
- Kim, K-H, Kim, BW, and Hong, SY (2019). "Experimental investigations on extreme bow-flare slamming loads of 10,000-TEU containership," *Ocean Eng*, 171, 225-240.
- Menter, FR (1994). "Two-equation eddy-viscosity turbulence models for engineering applications," *AIAA J*, 32(8), 1598-1605.
- Noack, R (2005). "SUGGAR: A general capability for moving body overset grid assembly," *AIAA Pap*, 5117.
- Shi, KY, Zhu, RC, Zheng, MM, and Li, CQ (2024). "Simulation of ship motion response in head seas using a fully nonlinear potential flow method," *Ocean Eng*, 309, 118309.
- Tezdogan, T, Incecik, A, and Turan, O (2016). "Full-scale unsteady RANS simulations of vertical ship motions in shallow water," *Ocean Eng*, 123, 131-145.
- Wang, A, Guo, H, Wang, JH, and Wan, DC (2023). "CFD Prediction of Slamming Loads on KCS in Oblique Waves," *Proc 33rd Int Offshore and Polar Eng Conf*, Ottawa, ISOPE-I-23-333.
- Xiao, Q, Zhu, RC, and Huang, S (2019). "Hybrid time-domain model for ship motions in nonlinear extreme waves using HOS method," *Ocean Eng*, 192, 106554.
- Xie, CM, Yang, JC, Sun, PN, Lyu, HG, Yu, J, and Ye, YL (2023). "An accurate and efficient HOS-meshfree CFD coupling method for simulating strong nonlinear wave-body interactions," *Ocean Eng*, 287, 115889.
- Yu, JW, Yao, CB, Wang, J, Liu, LW, Dong, GH, and Zhang, ZG (2023). "Numerical study on motion responses and added resistance for surge-free KCS in head and oblique waves based on the functional decomposition method," *Ocean Eng*, 285, 115300.
- Zhao, WW, Yang, XL, and Wan, DC (2024). "Numerical analysis of coupled sloshing and motion of a cylindrical FPSO in regular waves," *J Hydrodyn*, 36(3), 457-465.
- Zhuang, Y, Zhao, WW, and Wan, DC (2023a). "The Nonlinearity of Scattering Waves Due to Interaction between Focusing Waves and Floating Production Storage and Offloading," *Phys Fluids*, 35(10): 107113.
- Zhuang, Y, Zhou, FC, Zhou, WJ, and Wan, DC (2023b). "Numerical investigations of focused wave interact with a moving cylinder," *J Hydrodyn*, 35(4), 724-735.